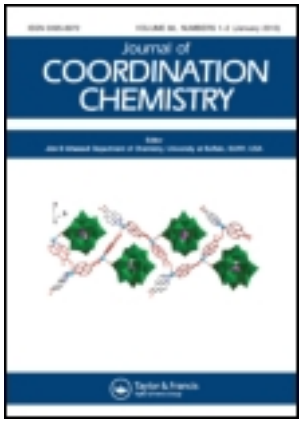

Journal of Coordination Chemistry
Publication details, including instructions for authors and subscription information:
http://www.tandfonline.com/loi/gcoo20

Syntheses, structural determination, and binding studies of nine-coordinate multinuclear $(mnH)_2[Eu^{III}(egta)]_2 \cdot 6H_2O$ and binuclear $(mnH)_4[Eu^{III}_2(dtpa)_2] \cdot 6H_2O$

Congcong Ma[a], Ying Li[a], Jun Wang[a], Jingqun Gao[a] & Qiong Wu[a]
[a] College of Chemistry, Liaoning University, Shenyang, P.R. China
Accepted author version posted online: 03 Oct 2013.Published online: 06 Nov 2013.

To cite this article: Congcong Ma, Ying Li, Jun Wang, Jingqun Gao & Qiong Wu (2013) Syntheses, structural determination, and binding studies of nine-coordinate multinuclear $(mnH)_2[Eu^{III}(egta)]_2 \cdot 6H_2O$ and binuclear $(mnH)_4[Eu^{III}_2(dtpa)_2] \cdot 6H_2O$, Journal of Coordination Chemistry, 66:20, 3660-3672, DOI: 10.1080/00958972.2013.850677

To link to this article: http://dx.doi.org/10.1080/00958972.2013.850677

Journal of Coordination Chemistry, 2013
Vol. 66, No. 20, 3660–3672, http://dx.doi.org/10.1080/00958972.2013.850677

Syntheses, structural determination, and binding studies of nine-coordinate multinuclear $(mnH)_2[Eu^{III}(egta)]_2 \cdot 6H_2O$ and binuclear $(mnH)_4[Eu^{III}_2(dtpa)_2] \cdot 6H_2O$

CONGCONG MA, YING LI, JUN WANG*, JINGQUN GAO and QIONG WU

College of Chemistry, Liaoning University, Shenyang, P.R. China

(*Received 14 July 2013; accepted 18 September 2013*)

Two lanthanide complexes, $(mnH)_2[Eu^{III}(egta)]_2 \cdot 6H_2O$ (**1**) (H_4egta = ethyleneglycol-bis-(2aminoethylether)-*N,N,N′,N′*-tetraacetic acid) and $(mnH)_4[Eu^{III}_2(dtpa)_2] \cdot 6H_2O$ (**2**) (H_5dtpa = diethylenetriamine-*N,N,N′,N″,N″*-pentaacetic acid), have been synthesized and characterized by FT-IR spectroscopy, thermal analysis, and single-crystal X-ray diffraction. X-ray diffraction reveals that **1** is multinuclear nine-coordinate and crystallizes in the monoclinic crystal system with space group *C2/c*. The obtained cell dimensions are a = 38.513(3) Å, b = 13.5877(8) Å, c = 8.7051(5) Å, β = 99.6780(10)°, and 4490.6(5) Å^3. Each methylamine (mnH^+) cation in **1**, through hydrogen bonds, connects three adjacent $[Eu^{III}(egta)]^-$ anions. The $[Eu^{III}(egta)]^-$ anions connect one another forming a 1-D multinuclear zigzag chain structure along the *c*-axis. Complex **2** is nine-coordinate binuclear structure with tricapped trigonal prismatic conformation and crystallizing in the monoclinic crystal system, but with space group $P2_1/n$. The obtained cell dimensions are a = 9.9132(8) Å, b = 24.1027(18) Å, c = 10.7120(10) Å, β = 109.1220(10)°, and 2418.2(3) Å^3. For **2**, there are two kinds of methylamine cations (mnH^+) connecting $[Eu^{III}_2(dtpa)_2]^{4-}$ complex anions and lattice waters through hydrogen bonds, leading to formation of a 2-D ladder-like layer structure.

Keywords: Eu^{III}; Ethyleneglycol-bis-(2-aminoethylether)-*N,N,N′,N′*-tetraacetic acid (H_4egta); Diethylenetriamine-*N,N,N′,N″,N″*-pentaacetic acid (H_5dtpa); Methylamine (mn); Hydrogen bond

1. Introduction

Design and construction of rare-earth metal complexes are of interest because of their intriguing structures, potential applications, strong magnetic properties, capacity for gas storage, ionic fluorescence, etc. [1–5]. For instance, Nd^{III} complexes have good anti-inflammation activity and Gd^{III} complexes have been used as contrast agents in magnetic resonance imaging (MRI) [6]. Pr^{III} complex in solids has showed outstanding optical features [7, 8]. Er^{III} and Tb^{III} have also been used as near infrared (NIR) luminescent rare-earth metal ions [9]. As a radioactive drug, some $^{153}Sm^{III}$ complexes have been clinically used to treat osteosarcoma [10, 11].

Many desired architectures have been generated through hydrothermal synthesis for formation of coordination bonds between ligands and metal centers. Numerous examples

*Corresponding author. Email: wangjuncomplex890@126.com

of rationally designed 1-D, 2-D, and 3-D structures via functional ligands have been reported [12–14]. We have worked hard in this field and have synthesized multidimensional coordination complexes [15, 16]. One of the many features that may be critical for the practical applications of coordination polymers is the high coordination number of the rare-earth metal ions, which renders structural flexibility and often increases the thermal stability. Aminopolycarboxylic acids can form extraordinarily stable and water-soluble complexes with various metal ions [17, 18]. Characteristics of lanthanide ions with N and O donors, coming from aminopolycarboxylic acids, may provide a new approach for construction of multidimensional coordination frameworks with useful chemical properties [19]. A series of Eu^{III} complexes coordinated with aminopolycarboxylic acid ligands, H_4egta (ethyleneglycol-bis-(2-aminoethylether)-*N,N,N′,N′*-tetraacetic acid) and H_5dtpa (diethylenetriamine-*N,N,N′,N″,N″*-pentaacetic acid), have been reported by our laboratory, such as $(en)_2[Eu^{III}(egta)]_2\cdot 6H_2O$ [20], $K_2[Eu^{III}(dtpa)(H_2O)]\cdot 5H_2O$ [21], $Na_4[Eu^{III}(dtpa)(H_2O)]_2\cdot 11.5H_2O$, and $(NH_4)_4[Eu^{III}(dtpa)]_2\cdot 10H_2O$ [22]. By comparative analysis, we found that $(en)_2[Eu^{III}(egta)]_2\cdot 6H_2O$, $Na_4[Eu^{III}(dtpa)(H_2O)]_2\cdot 11.5H_2O$, and $K_2[Eu^{III}(dtpa)(H_2O)]\cdot 5H_2O$ are nine-coordinate mononuclear complexes, but $(NH_4)_4[Eu^{III}(dtpa)]_2\cdot 10H_2O$ is a nine-coordinate binuclear complex. Although the Eu^{III}-egta and Eu^{III}-dtpa complexes with various counter ions all adopt nine-coordinate structures, variability exists in their molecular structures. Their coordinate structures and molecular structures sometimes are related to the shape of ligands and also the counter ion species. We want to know how organic amine and ligand species generate effects upon coordination number, coordination structure, space group, molecular structure, and crystal structure.

We chose two aminopolycarboxylic acids, H_4egta (ethyleneglycol-bis-(2-aminoethylether)-*N,N,N′,N′*-tetraacetic acid) and H_5dtpa (diethylenetriamine-*N,N,N′,N″,N″*-pentaacetic acid), as ligand and methylamine (mn) as counter ion. Two coordination polymers, $(mnH)_2[Eu^{III}(egta)]_2\cdot 6H_2O$ (**1**) and $(mnH)_4[Eu^{III}{}_2(dtpa)_2]\cdot 6H_2O$ (**2**), have been obtained under hydrothermal synthesis. Single-crystal X-ray diffraction reveals that they both adopt nine-coordinate structures. However, due to different ligands as well as choosing methylamine as counter ion, their molecular structures are different. We conclude that the ligand structures and the counter ions have a crucial effect on the molecular and crystal structures of rare-earth metal complexes with aminopolycarboxylic acid ligands.

2. Experimental

2.1. *Syntheses*

2.1.1. $(mnH)_2[Eu^{III}(egta)]_2\cdot 6H_2O$ (1). H_4egta (A.R., Beijing SHLHT Science & Trade Co., Ltd, China) (1.9017 g, 5.0 mM) was added to 100 mL warm water and Eu_2O_3 powder (99.999%, Yuelong Rare Earth Co., Ltd, China) (0.8797 g, 2.5 mM) was slowly added to the solution. The solution became transparent after the mixture had been stirred and refluxed for 15.0 h, and then the pH was adjusted to 6.0 by dilute methylamine (mn) aqueous solution. Finally, the solution was concentrated to 25 mL. White crystals appeared after three weeks at room temperature.

2.1.2. $(mnH)_4[Eu^{III}{}_2(dtpa)_2]\cdot 6H_2O$ (2). H_5dtpa (A.R., Beijing SHLHT Science & Trade Co., Ltd, China) (1.9668 g, 5.0 mM) was added to 100 mL warm water and Eu_2O_3 powder (99.999%, Yuelong Rare Earth Co., Ltd, China) (0.8797 g, 2.5 mM) was slowly added.

After the mixture had been stirred and refluxed for 18.0 h, the solution became transparent and the pH was adjusted to 6.0 by dilute methylamine (mn) aqueous solution. Finally, the solution was concentrated to 25 mL. Light yellow crystals appeared after two weeks at room temperature.

2.2. *FT-IR spectroscopy*

The H_4egta, H_5dtpa, $(mnH)_2[Eu^{III}(egta)]_2{\cdot}6H_2O$ (**1**), and $(mnH)_4[Eu^{III}_2(dtpa)_2]{\cdot}6H_2O$ (**2**) samples were skived and pressed to slices with KBr, respectively, and their FT-IR spectra were determined by a Schimadzu-IR 408 spectrophotometer (Schimadzu company, Japan). The obtained results are shown in figure S1.

2.3. *Determination of TG-DTA*

Thermal analyses of the two complexes, $(mnH)_2[Eu^{III}(egta)]_2{\cdot}6H_2O$ (**1**) and $(mnH)_4[Eu^{III}_2(dtpa)_2]{\cdot}6H_2O$ (**2**), were conducted using a Mettler-Toledo 851° thermogravimetric analyzer (Mettler-Toledo company, Switzerland) in a flow of Ar (20 mL min^{-1}) from room temperature to 800 °C at a heating rate of 20 °C min^{-1}. The thermograms are shown in figure S2.

2.4. *X-ray structure determination*

X-ray intensity data were collected on a Bruker SMART CCD type X-ray diffractometer system with graphite-monochromated Mo Kα radiation ($\lambda = 0.71073$ Å) at 298 K using φ–ω scan technique in the range of $1.72° \le \theta \le 26.00°$. The structures were solved by direct methods. All non-hydrogen atoms were refined anisotropically by full-matrix least squares methods. All the calculations were performed by the SHELXTL-97 program on PDP11/44 and Pentium MMX/166 computers. The crystal data and structure refinements for **1** and **2** are listed in table 1. Final atomic coordinates and equivalent isotropic displacement parameters for all the non-hydrogen fractions are presented in Supplementary material. Selected bond distances and angles of **1** and **2** are listed in table 2. Hydrogen bond distances (Å) and angles of **1** and **2** are listed in table 3.

3. Results and discussion

3.1. *FT-IR spectroscopy*

3.1.1. $(mnH)_2[Eu^{III}(egta)]_2{\cdot}6H_2O$ (1). Figure S1(I) reveals the comparison of FT-IR spectra between H_4egta and **1**. That $\nu_{(C-N)}$ of **1** appears at 1069 cm^{-1}, displays a red shift (66 cm^{-1}) compared with $\nu_{(C-N)}$ of H_4egta at 1135 cm^{-1}, which demonstrates that the amine nitrogens of H_4egta coordinate to Eu^{III}. The spectrum of free H_4egta shows a strong band at 1743 cm^{-1} originating from ν(C=O), which disappears completely in the FT-IR spectrum of **1**. **1** shows the characteristic absorption peaks of carboxyl at 1604 cm^{-1} for the asymmetric stretch and at 1408 cm^{-1} for the symmetric stretch, revealing a red shift (34 cm^{-1}) compared with 1638 cm^{-1} of H_4egta and a blue shift of 9 cm^{-1} compared with 1399 cm^{-1} of H_4egta. These changes demonstrate that oxygen of carboxyl are also coordinated to

Table 1. Crystal data and structure refinements for $(mnH)_2[Eu^{III}(Egta)]_2{\cdot}6H_2O$ (**1**) and $(mnH)_4[Eu^{III}_2(dtpa)_2]{\cdot}6H_2O$ (**2**).

Complex	**1**	**2**
Formula weight	1228.79	1316.92
Temperature, K	298(2)	298(2)
Wavelength, Å	0.71073	0.71073
Crystal system	Monoclinic	Monoclinic
Space group	*C2/c*	*P2*(1)*/n*
Unit cell dimensions		
a, Å	38.513(3)	9.9132(8)
b, Å	13.5877(8)	24.1027(18)
c, Å	8.7051(5)	10.7120(10)
β, °	99.6780(10)	109.1220(10)
Volume, $Å^3$	4490.6(5)	2418.2(3)
Z	4	2
ρ_{Calcd}, mg/m^3	1.818	1.809
Absorption coefficient, mm^{-1}	2.864	2.668
F(000)	2480	1336
Crystal size, mm	0.18 × 0.09 × 0.06	0.28 × 0.18 × 0.16
θ_{range} for data collection, °	2.20–25.01	2.33–25.02
Limiting indices	$-23 \le h \le 45$ $-16 \le k \le 16$ $-10 \le l \le 10$	$-11 \le h \le 11$ $-23 \le k \le 28$ $-12 \le l \le 12$
Reflections collected	11,664	11,644
Independent reflections	3962 [R(int) = 0.0936]	4225 [R(int) = 0.0387]
Completeness to θ_{max}, %	99.8	99.0
Max. and min. transmission	0.8470 and 0.6267	0.6749 and 0.5221
Goodness-of-fit on F^2	1.018	1.202
Final R indices [$I > 2\sigma(I)$]	$R_1 = 0.0442$, w$R_2 = 0.0930$	$R_1 = 0.0529$ w$R_2 = 0.1530$
R indices (all data)	$R_1 = 0.0726$, w$R_2 = 0.1019$	$R_1 = 0.0627$, w$R_2 = 0.1598$
Largest difference peak and hole $eÅ^{-3}$	1.437 and −1.106	1.427 and −2.093
Absorption correction	Empirical	
Refinement method	Full-matrix least squares on F^2	

Eu^{III}. The broad absorption at 3436 cm^{-1} for **1** could be reasonably attributed to the stretching vibration of O–H.

3.1.2. $(mnH)_4[Eu^{III}_2(dtpa)_2]{\cdot}6H_2O$ (2). Comparison of FT-IR spectra between H_5dtpa and **2** are shown in figure S1(II). The IR spectrum shows ν(C–N) at 928 cm^{-1}, a red-shift (33 cm^{-1}) compared with $\nu_{(C–N)}$ of H_5dtpa at 961 cm^{-1} indicating coordination of nitrogen. The spectrum of free H_5dtpa shows a strong band at 1734 cm^{-1} of ν(C=O), which disappears completely in **2**. Carboxyl groups are at 1594 cm^{-1} for the asymmetric stretch and at 1409 cm^{-1} for the symmetric stretch, with the separation value (Dt) of 185 cm^{-1} for ν_{as}(OCO) and ν_s(OCO). These results clearly show that oxygens in carboxylate participate in coordination to Eu^{III}. The broad absorption at 3443 cm^{-1} for **2** could be the stretch of O–H.

3.2. *Thermal analyzes*

3.2.1. $(mnH)_2[Eu^{III}(egta)]_2{\cdot}6H_2O$ (1). As shown in figure S2, the TG curve of **1** shows a three-stage decomposition pattern. The first weight loss is 6.5% from room temperature to 125 °C corresponding to releases of methylamine, with two endothermic peaks at 70 and 110 °C in the DTA curve. The second weight loss of 8.9% from 125 to 282 °C corresponds

Table 2. Selected bond distances (Å) and angles (deg) of **1** and **2** (symmetry code: #1: x, $1-y$, $z-1/2$).

Bond	d, Å	Bond	d, Å	Bond	d, Å
1					
Eu(1)–O(1)	2.498(5)	Eu(1)–O(5)	2.382(5)	Eu(1)–O(10)#1	2.361(5)
Eu(1)–O(2)	2.506(5)	Eu(1)–O(7)	2.419(5)	Eu(1)–N(1)	2.604(6)
Eu(1)–O(3)	2.382(5)	Eu(1)–O(9)	2.321(5)	Eu(1)–N(2)	2.656(6)
2					
Eu(1)–O(1)	2.369(6)	Eu(1)–O(5)	2.373(6)	Eu(1)–N(1)	2.787(7)
Eu(1)–O(3)	2.472(5)	Eu(1)–O(7)	2.364(5)	Eu(1)–N(2)	2.637(6)
Eu(1)–O(4)	2.463(5)	Eu(1)–O(9)	2.442(5)	Eu(1)–N(3)	2.645(6)
Angle	ω, deg	Angle	ω, deg	Angle	ω, deg
1					
O(1)–Eu(1)–O(2)	66.65(16)	O(2)–Eu(1)–O(10)#1	67.44(17)	O(5)–Eu(1)–N(1)	65.69(18)
O(1)–Eu(1)–O(3)	124.19(17)	O(2)–Eu(1)–N(1)	132.07(18)	O(5)–Eu(1)–N(2)	135.58(19)
O(1)–Eu(1)–O(5)	102.18(18)	O(2)–Eu(1)–N(2)	66.98(17)	O(7)–Eu(1)–O(9)	128.81(16)
O(1)–Eu(1)–O(7)	69.50(16)	O(3)–Eu(1)–O(5)	82.38(18)	O(7)–Eu(1)–O(10)#1	133.94(17)
O(1)–Eu(1)–O(9)	151.62(17)	O(3)–Eu(1)–O(7)	75.66(17)	O(7)–Eu(1)–N(1)	79.67(17)
O(1)–Eu(1)–O(10)#1	75.69(17)	O(3)–Eu(1)–O(9)	83.79(18)	O(7)–Eu(1)–N(2)	64.44(17)
O(1)-Eu(1)–N(1)	67.70(18)	O(3)–Eu(1)–O(10)#1	150.39(18)	O(9)–Eu(1)–O(10)#1	76.70(16)
O(1)–Eu(1)–N(2)	122.17(19)	O(3)–Eu(1)–N(1)	64.14(18)	O(9)–Eu(1)–N(1)	131.11(19)
O(2)–Eu(1)–O(3)	137.81(17)	O(3)–Eu(1)–N(2)	75.35(18)	O(9)–Eu(1)–N(2)	65.15(17)
O(2)–Eu(1)–O(5)	138.61(17)	O(5)–Eu(1)–O(7)	144.54(17)	O(10)#1-Eu(1)-N(1)	113.86(18)
O(2)–Eu(1)–O(7)	71.52(17)	O(5)–Eu(1)–O(9)	74.71(17)	O(10)#1-Eu(1)-N(2)	114.77(18)
O(2)–Eu(1)–O(9)	96.61(17)	O(5)–Eu(1)–O(10)#1	71.19(18)	N(1)–Eu(1)–N(2)	131.25(18)
2					
O(1)–Eu(1)-O(3)	77.25(19)	O(3)–Eu(1)–N(1)	60.57(17)	O(5)–Eu(1)–N(2)	67.57(19)
O(1)–Eu(1)–O(4)	132.5(2)	O(3)–Eu(1)–N(2)	127.61(18)	O(5)–Eu(1)–N(3)	127.95(19)
O(1)–Eu(1)–O(5)	133.4(2)	O(3)–Eu(1)–N(3)	141.79(19)	O(7)–Eu(1)–O(9)	89.67(19)
O(1)–Eu(1)–O(7)	135.81(19)	O(4)–Eu(1)–O(5)	80.88(19)	O(7)–Eu(1)–N(1)	138.2(2)
O(1)–Eu(1)–O(9)	72.95(19)	O(4)–Eu(1)–O(7)	74.59(19)	O(7)–Eu(1)–N(2)	76.5(2)
O(1)–Eu(1)–N(1)	63.42(19)	O(4)–Eu(1)–O(9)	71.98(19)	O(7)–Eu(1)–N(1)	66.17(19)
O(1)–Eu(1)–N(2)	86.3(2)	O(4)–Eu(1)–N(1)	123.33(17)	O(9)–Eu(1)–N(1)	130.55(19)
O(1)–Eu(1)–N(3)	66.17(19)	O(4)–Eu(1)–N(2)	141.3(2)	O(9)–Eu(1)–N(2)	132.98(18)
O(3)–Eu(1)–O(4)	71.02(18)	O(4)–Eu(1)–N(3)	119.33(19)	O(9)–Eu(1)–N(3)	63.75(18)
O(3)–Eu(1)–O(5)	88.84(18)	O(5)–Eu(1)–O(7)	76.2(2)	N(1)–Eu(1)–N(2)	67.52(19)
O(3)–Eu(1)–O(7)	144.23(19)	O(5)–Eu(1)–O(9)	151.96(19)	N(1)–Eu(1)–N(3)	116.82(19)
O(3)–Eu(1)–O(9)	88.90(17)	O(5)–Eu(1)–N(1)	71.0(2)	N(2)–Eu(1)–N(3)	69.58(19)

Table 3. Hydrogen bond distances (Å), bond angles (deg), and symmetry codes of **1** and **2**.

D–H	d(D–H)	d(H···A)	∠ DHA	d(D···A)	A	Symmetry code
1						
N(3)–H(3A)	0.890	1.892	157.87	2.737	O(6)	$x, y, z+1$
N(3)–H(3B)	0.890	1.987	169.46	2.866	O(3)	$-x+1/2, y, -z+3/2$
N(3)–H(3C)	0.890	1.964	160.41	2.818	O(5)	$-x+1, -y+1, -z+1$
2						
N(4)–H(4A)	0.890	2.128	149.52	2.930	O(5)	
N(4)–H(4A)	0.890	2.485	114.62	2.968	O(3)	$-x+1, -y+1, -z+1$
N(4)–H(4B)	0.890	1.998	168.50	2.876	O(9)	$-x+1, -y+1, -z+1$
N(4)–H(4C)	0.890	1.887	166.01	2.759	O(10)	$x+1, y, z$
N(5)–H(5A)	0.890	1.948	163.87	2.814	O(13)	$x, y, z+1$
N(5)–H(5B))	0.890	2.155	147.17	2.942	O(11)	$x, y, z+1$
N(5)–H(5B)	0.890	2.641	121.81	3.201	O(11)	$-x+1, -y+1, -z+1$
N(5)–H(5C)	0.890	1.991	169.75	2.872	O(7)	
N(5)–H(5C)	0.890	2.557	130.90	3.211	O(8)	

to the expulsion of six lattice waters, with a marked endothermic peak at 248 °C. Then, sample decomposes gradually, completed at 800 °C; the corresponding weight loss is 48%, with a series of exothermic peaks at 370, 450, 650, and 580 °C. The final residue is mainly Eu_2O_3 and the overall weight loss ratio is about 63.4%.

3.2.2. $(mnH)_4[Eu^{III}_2(dtpa)_2]\cdot 6H_2O$ (2). As shown in figure S2, **2** displays similar thermal behavior. The first stage weight loss is 9.3% from room temperature to 148 °C, which corresponds to expulsion of methylamine. There are marked endothermic peaks in the DTA curve at 32 and 130 °C. From 148 to 220 °C, the weight loss is very small, indicating that the crystal structure is very stable, and did not collapse until 220 °C. The second stage weight loss of 13.5% from 220 to 295 °C attributed to expulsion of lattice water produces a DTA peak located at 275 °C. The last weight loss of 47.5% occurs from 295 to 800 °C, which is attributed to decomposition and combustion of carboxylate, with exothermic peaks at 395, 510, 540, and 610 °C, respectively. The final residue is mainly Eu_2O_3 and the total weight loss is 70.3%.

3.3. *Molecular and crystal structures*

3.3.1. $(mnH)_2[Eu^{III}(egta)]_2\cdot 6H_2O$ (1). Figure 1 shows the nine-coordinate structure of **1** with a 1 : 1 metal to ligand stoichiometry. In the asymmetry unit of **1**, Eu^{III} is nine-coordinate environment with two amine N and seven O, in which O($10^{\#}$) belongs to carboxyl (O($9^{\#}$)–C($13^{\#}$)–O($10^{\#}$)) from another egta. The remaining two amine N, four carboxyl O, and two ethyleneglycol O atoms come from one octadentate egta ligand. O(10) connecting to another Eu^{III} causes formation of a 1-D multinuclear zigzag chain along the *c*-axis (shown in figure 2). Due to steric hindrance, the molecules slightly rotate along the *b*-axis.

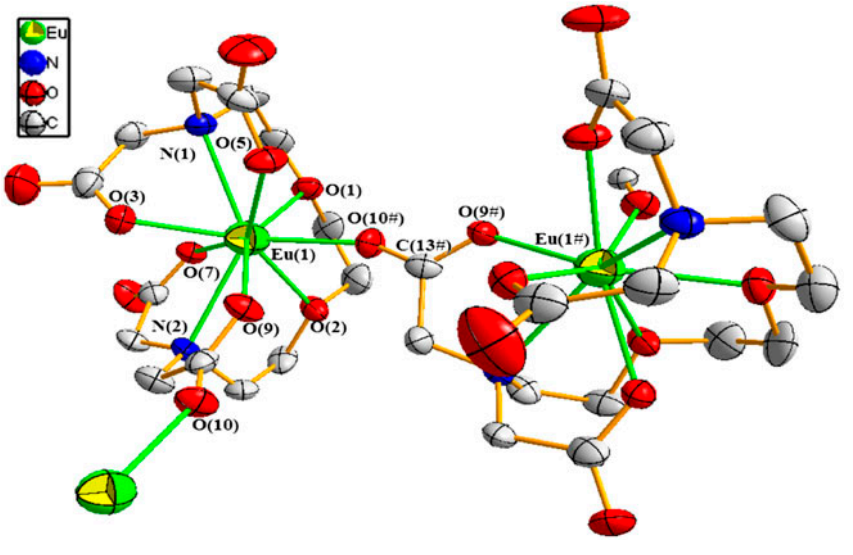

Figure 1. Molecular structure of **1**.

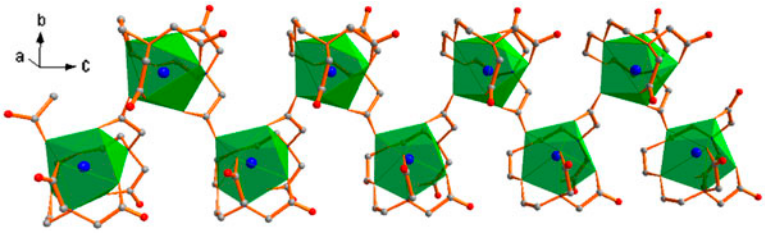

Figure 2. 1-D multinuclear zigzag chain structure along the *c*-axis of **1**.

As shown in figure 3, the coordinate geometry around Eu^{III} in EuN_2O_7 can thus be considered as nine-coordinate distorted monocapped square antiprismatic (MC-SAP) conformation. The upper square plane is formed by one ethyleneglycol O (O(2)) and three carboxyl O(3), O(7), and O(9) and the lower plane is formed by one amine N(1), one ethyleneglycol O(1), one carboxyl O(5), and one carboxyl O($10^{\#}$) from another egta. The capping donor is occupied by one N(2). The torsion angle between the two (upper and lower) quadrilateral planes is 42.25°.

It can also be calculated (figure 3) that, to the upper quadrilateral plane, the value of the trigonal dihedral angle between Δ(O(2)O(3)O(9)) and Δ(O(2)O(3)O(7)) is 12.87°, and between Δ(O(2)O(7)O(9)) and Δ(O(3)O(7)O(9)) is 11.81°. To the bottom quadrilateral plane, the trigonal dihedral angle between Δ(O(1)O(5)O($10^{\#}$)) and Δ(O(1)O(5)N(1)) is 9.25°, and between Δ(O(1)O($10^{\#}$)N(1)) and Δ(O(5)O($10^{\#}$)N(1)) is 10.17°. According to the

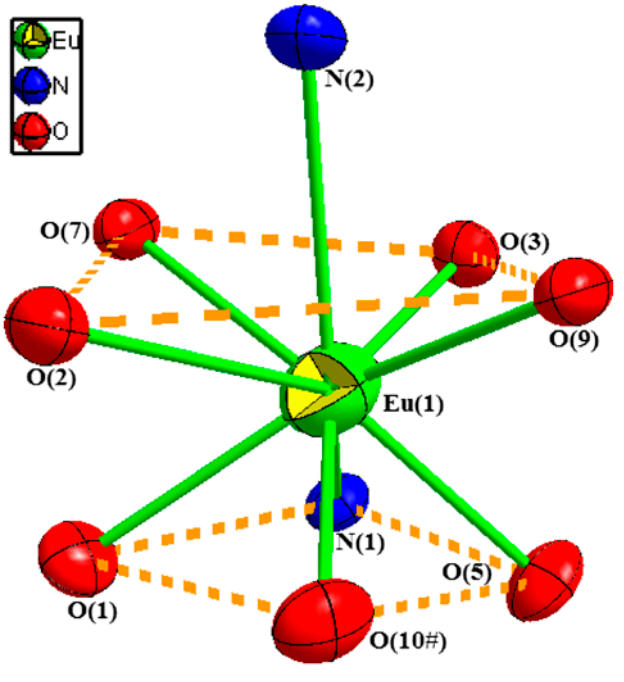

Figure 3. Coordination polyhedron around Eu(1) in **1**.

viewpoint of Guggenberger and Muetterties [23], if the dihedral angle for nine-coordinate lanthanide complexes is between 0° and 26.4° the coordinate conformation can be regarded as pseudo-monocapped square antiprism. For this reason, it can be firmly concluded that EuN_2O_7 has a nine-coordinate monocapped square antiprism (MC-SAP) but distorted slightly.

As shown in table 2, the Eu(1)–O bond distances are considerably different, in the range of 2.321(5) Å (Eu(1)–O(9)) to 2.506(5) Å (Eu(1)–O(2)), and the average value is about 2.410(5) Å. Eu(1)–O(1) and Eu(1)–O(2) bond distances (both belonging to ethyleneglycol) are somewhat longer than other Eu(1)–O bond lengths, consistent with findings with H_4egta made previously [24, 25]. The two Eu(1)–N bond distances are 2.604(6) Å (Eu(1)–N(1)) and 2.656(6) Å (Eu(1)–N(2)), respectively, with the average value of 2.630(6) Å. The Eu(1)–O bond distances are significantly shorter than Eu(1)–N bond distances, indicating that Eu(1)–O bonds are stronger than Eu(1)–N bonds. The distorted geometric configuration of $(mnH)_2[Eu^{III}(egta)]_2\cdot 6H_2O$ is shown by O–Eu–O bond angles from 66.65(27)° (∠O(1)–Eu(1)–O(9)) to 151.62(16)° (∠O(1)–Eu(1)–O(2)), while the O–Eu–N bond angles vary from 64.14(18)° (∠O(3)–Eu(1)–N(1)) to 135.58(19)° (O(5)–Eu(1)–N(2)), and the N(1)–Eu–N(2) bond angle is 131.25(18)°.

As shown in figure 4, there are four $(mnH)_2[Eu^{III}(egta)]_2\cdot 6H_2O$ molecules in a unit cell. The molecules connect with crystal water and protonated methylamine cations (mnH^+) through hydrogen bonds and crystallize in a monoclinic system with *C2/c* space group. As seen from figure 5, the mnH^+ forms hydrogen bonds with three adjacent $[Eu^{III}(egta)]^-$ anions. Every N(3) connects three carboxyl O, in which O(3) and O(5) are coordinated carboxyl, while O(6) is uncoordinated. They come from three different $[Eu^{III}(egta)]^-$ anions, respectively. The hydrogen bond distances of N(3)···O(3), N(3)···O(5), and N(3)···O(6) are 2.866, 2.818, and 2.737 Å (shown in table 3), respectively.

Every 1-D multinuclear zigzag chain connects to another by water molecules along the *bc* plane, leading to a 2-D ladder-like network. The 2-D ladder-like network is further consolidated via weak hydrogen bonds between water and carboxyl oxygen and nitrogen from methylamine to extend into a 3-D double-deck cage-like structure in *ab* plane. Due to

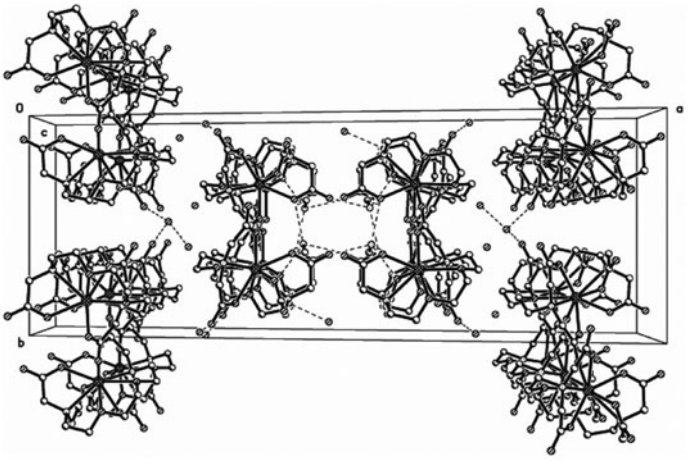

Figure 4. Arrangement of **1** in the unit cell (dashed lines represent intermolecular hydrogen bonds).

steric hindrance, the relation between the two planes is center symmetric. One double-deck cage-like structure acts as a unit, and two such units are linked by electrostatic force along the *a* axis which strengthens the structure.

3.3.2. $(mnH)_4[Eu^{III}_2(dtpa)_2]\cdot 6H_2O$ (2). As seen from figure 6, in **2**, Eu^{III} is nine-coordinate like most aminopolycarboxylic acid ligands [26, 27]. **2** has a binuclear molecular structure, in which every Eu^{III} is nine-coordinate with three nitrogens and five carboxylate oxygens, from one dtpa ligand, and another oxygen from another dtpa. For $[Eu^{III}_2(dtpa)_2]^{4-}$, Eu(1) and Eu($1^{\#}$) are centrosymmetric and the symmetric center is located at the point of intersection of the two diagonals of the parallelogram formed by Eu(1), O(4), Eu($1^{\#}$), and O($4^{\#}$) (symmetry code: $1^{\#}$: $-x + 1, -y + 1, -z + 1$). As an octadentate ligand, dtpa is not able to supply a sufficient number of donor atoms to fill all coordination positions around Eu^{III}. Each dtpa is coordinated to Eu(1) using its five carboxylic oxygens and three amine nitrogens, while the sixth oxygen, O($4^{\#}$), is used to form an additional coordination bond to Eu($1^{\#}$). Therefore, O(4) and its symmetry equivalent O($4^{\#}$) play a role in connecting Eu(1) and Eu($1^{\#}$). In fact, the O(3)–C(7)–O($4^{\#}$) and O($3^{\#}$)–C($7^{\#}$)–O(4) carboxylates connect Eu(1) and Eu($1^{\#}$). Seven five-membered rings are formed in Eu(1) and Eu($1^{\#}$) with the atoms of each ring being almost coplanar.

As seen from figure 7, the coordination polyhedron of $[Eu^{III}_2(dtpa)_2]^{4-}$ is nine-coordinate pseudo-tricapped trigonal prismatic (TC-TP) conformation. The upper triangular plane is formed by three carboxyl O(1), O(3), and O(9), while the lower triangular plane is formed by carboxyl O(5) and O(7) and one amine nitrogen N(2). The first square plane is formed by three carboxyl O(1), O(3), and O(5) and one amine N(2). The second square plane is formed by three carboxyl O(1), O(9), and O(7) and one amine N(2). The third square plane is formed by four carboxyl O(3), O(5), O(7), and O(9). For these three square planes, the capping positions are occupied by two amine N(1) and N(3) and one carboxyl O(4), respectively.

As shown in table 2, the Eu(1)–O bond distances in $(mnH)_4[Eu^{III}_2(dtpa)_2]\cdot 6H_2O$ are 2.364(5) Å (Eu(1)–O(5)) to 2.472(5) Å (Eu(1)–O(3)), with average value of 2.414(4) Å. Eu

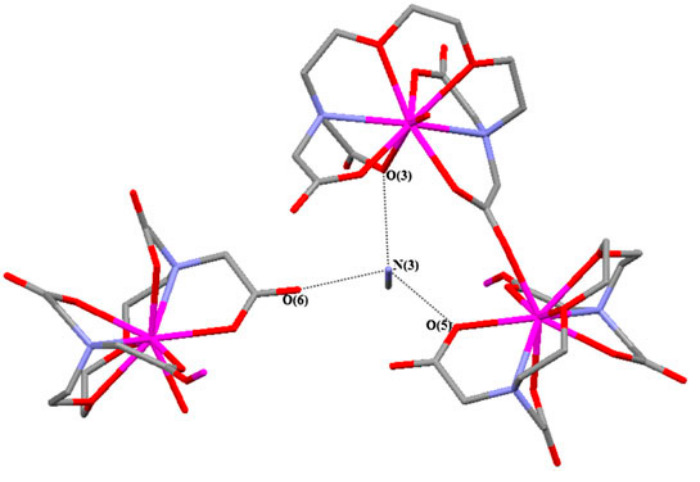

Figure 5. Inner hydrogen bonds in **1**.

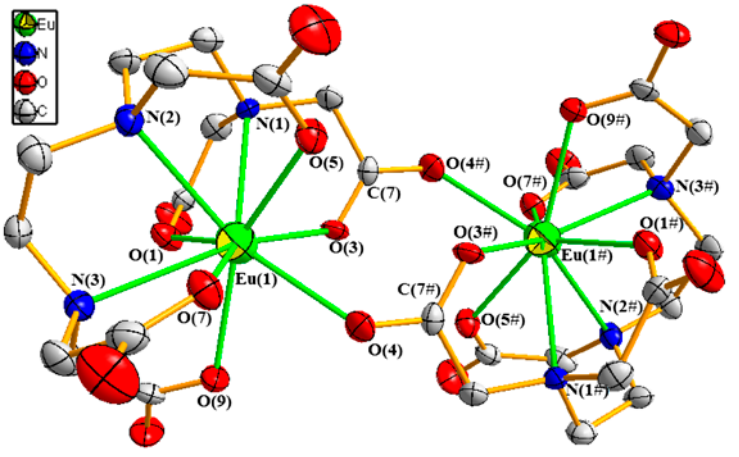

Figure 6. Molecular structure of **2**.

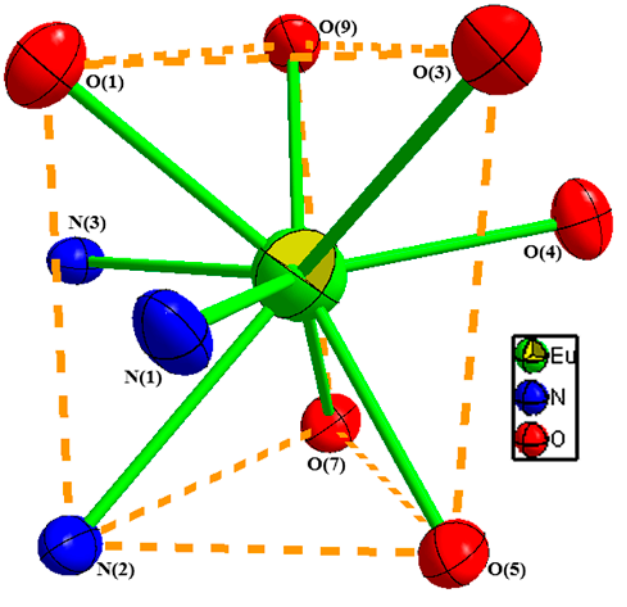

Figure 7. Coordination polyhedron around Eu(1) in **2**.

(1)–N bond distances varying from 2.637(6) Å (Eu(1)–N(2)) to 2.787(7) Å (Eu(1)–N(1)), with average value of 2.690(3) Å, remarkably longer than the Eu(1)–O bond distances. The O–Eu(1)–O bond angles are 71.02(18)° (∠O(3)–Eu(1)–O(4)) to 151.96(19)° (∠O(5)–Eu (1)–O(9)), the O–Eu(1)–N bond angles vary from 60.57(17)° (∠O(3)–Eu(1)–N(1)) to 141.79(19)° (∠O(3)–Eu(1)–N(3)), and the ∠N–Eu(1)–N bond angles change from 67.52 (19)° (N(1)–Eu(1)–N(2)) to 116.82(19)° (N(1)–Eu(1)–N(3)). The smallest and largest bond angles are 60.57(17)° (∠O(3)–Eu(1)–N(1)) and 151.96(19)° (∠O(5)–Eu(1)–O(9)), respectively.

Because of the repulsion between the capped atoms (O(4), N(1), and N(3)) and the planes (formed by O(1), O(3), O(5), and N(2), O(1), O(7), O(9), and N(2) and O(3), O(5), O(7), and O(9)) (figure 7), Eu(1)N_3O_6 is not a standard tricapped trigonal prismatic conformation. To the O(1)O(3)O(5)N(2) square plane, the value of trigonal dihedral angle is 10.01° between Δ(O(1)O(3)O(5)) and Δ(O(1)N(2)O(5)) and 10.55° between Δ(O(3)O(5)N(2)) and Δ(O(3)O(1)N(2)). To the O(1)O(7)O(9)N(2) square plane, the trigonal dihedral angle between Δ(O(9)O(1)N(2)) and Δ(O(9)O(7)N(2)) is about 6.21° and between Δ(O(1)N(2)O(7)) and Δ(O(1)O(9)O(7)) is about 5.85°. To the O(3)O(5)O(7)O(9) square plane, the trigonal dihedral angle between Δ(O(3)O(9)O(7)) and Δ(O(3)O(5)O(7)) is about 7.81° and between Δ(O(5)O(3)O(9)) and Δ(O(5)O(7)O(9)) is about 7.93°. The values of the trigonal dihedral angle trend to 0°, showing four atoms are almost in the same plane. These data predict that four atoms of every side of a triangular prism are almost located in the same plane. We conclude that the conformation of Eu(1)N_3O_6 in **2** is a tricapped trigonal prismatic (TC-TP) conformation but distorted to a small extent.

There are two $(mnH)_4[Eu^{III}_2(dtpa)_2]\cdot 6H_2O$ (**2**) (figure 8) in a unit cell. The molecules connect with lattice water and protonated methylamine cations (mnH^+) through hydrogen bonds and crystallize in a monoclinic system with $P2_1/n$ space group. Hydrogen bonds play an important role in the construction of the 2D planar structure of **2**. There are two kinds of mnH^+ (figure S3), one mnH^+ is N(4)–C(15) which connects with four oxygens, O(3), O(5), and O(9), are coordinated carboxyl from one $(mnH)_4[Eu^{III}_2(dtpa)_2]\cdot 6H_2O$, and O(10) is uncoordinated carboxyl from the other $(mnH)_4[Eu^{III}_2(dtpa)_2]\cdot 6H_2O$. The hydrogen bond distances of N(4)···O(3), N(4)···O(5), N(4)···O(9), and N(4)···O(10) are 2.968, 2.930, 2.891, and 2.759 Å, respectively. The second mnH^+ is N(5)–C(16) which links one coordinated carboxyl O(7) from one $(mnH)_4[Eu^{III}_2(dtpa)_2]\cdot 6H_2O$ and O(11) and O(13) from two lattice waters. N(5)···O(7), N(5)···O(11), and N(5)···O(13) hydrogen bond distances are 2.872, 2.942, and 2.814 Å, respectively.

Two $[Eu^{III}_2(dtpa)_2]^{4-}$ are interconnected by methylamine (N(4)–C(15)) (figure S4), forming a basic secondary building unit (SBU). The two neighboring SBU are further connected by sharing methylamine (N(5)–C(16)) and water (O(11)) along the *c*-axis, with O(7)···N(5), O(11)···N(5) and O(11)···O(4) hydrogen bond distances of 2.872, 2.942, and 2.881 Å, respectively, resulting in an infinite 1-D chain; 1-D chains connect by water and methylamine along the *ac* plane, leading to a 2-D ladder-like network structure.

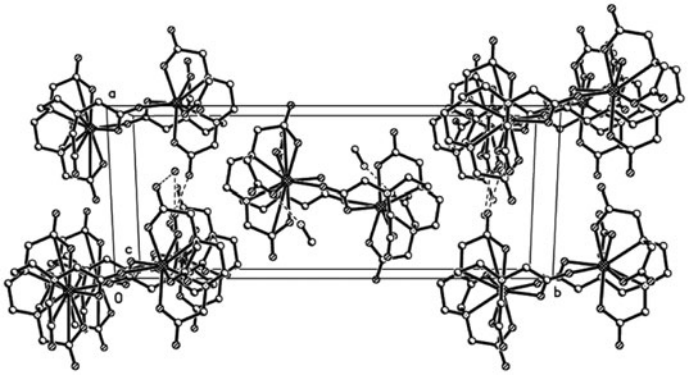

Figure 8. Arrangement of **2** in the unit cell (dashed lines represent intermolecular hydrogen bonds).

4. Conclusions

Two Eu^{III} complexes with aminopolycarboxylic acid ligands, $(mnH)_2[Eu^{III}(egta)]_2{\cdot}6H_2O$ (**1**) and $(mnH)_4[Eu^{III}_2(dtpa)_2]{\cdot}6H_2O$ (**2**), were synthesized and characterized by single-crystal X-ray diffraction, infrared spectra, and thermal analyses. The $(mnH)_2[Eu^{III}(egta)]_2{\cdot}6H_2O$ adopts a multinuclear nine-coordinate square antiprismatic polyhedron and crystallizes in the monoclinic crystal system with space group *C2/c*. The ammonium and ethylenediamine salts of rare-earth metal complexes with egta often possess a mononuclear nine-coordinate structure; however, being different from $(en)_2[Eu^{III}(egta)]_2{\cdot}6H_2O$, the use of methylamine as the counter ion results in the formation of the multinuclear structure of **1**. The $(mnH)_2[Eu^{III}(egta)]_2{\cdot}6H_2O$ connect forming a 1-D multinuclear zigzag chain structure along the *c*-axis. Most ammonium salts of rare-earth metal complexes with dtpa have binuclear nine-coordinate structures. **2** takes a binuclear nine-coordinate tricapped trigonal prismatic polyhedron and crystallizes in the monoclinic crystal system with space group $P2_1/n$. However, **2** is different from the previously reported $Na_4[Eu^{III}(dtpa)(H_2O)]_2{\cdot}11.5H_2O$, and $K_2[Eu^{III}(dtpa)(H_2O)]{\cdot}5H_2O$ and $[Eu^{III}_2(dtpa)_2]^{4-}$ have a 2-D ladder-like network structure through connection of mnH^+. The use of different ligands results in different crystal structures of the two Eu^{III} complexes. Thus, molecular and crystal structures of rare-earth complexes not only related to the shape of ligands, but also the counter ion species.

Supplementary material

CCDC 842912 $(mnH)_2[Eu^{III}(egta)]_2{\cdot}6H_2O$ and CCDC 947291 $(mnH)_4[Eu^{III}_2(dtpa)_2]{\cdot}6H_2O$ contain the supplementary crystallographic data for this article. These data can be obtained free of charge via www.ccdc.cam.ac.uk/data_request/cif, by e-mailing data_request@ccdc.cam.ac.uk, or by contacting The Cambridge Crystallographic Data Center, 12 Union Road, Cambridge CB2 1EZ, UK; Fax:+44(0)1223–336033. Supplemental data for this article can be accessed http://dx.doi.org/10.1080/00958972.2013.850677.

Acknowledgements

The authors greatly acknowledge the National Science Foundation of China (21371084), Liaoning Provincial Department of Education Innovation Team Projects (LT2012001), Shenyang Science and Technology Plan Projects (F12-277-1-15) and Liaoning University "211" Engineering Construction Projects for financial support. The authors also thank our colleagues and other students for their participation in this work.

References

[1] X.J. Gu, D.F. Xue. *Inorg. Chem.*, **45**, 9257 (2006).
[2] Y.J. Zhang, B.Q. Ma, S. Gao, J.R. Li, Q.D. Liu, G.H. Wen, X.X. Zhang. *J. Chem. Soc., Dalton Trans.*, 2249 (2000).
[3] J. Lisowski, P. Starynowicz. *Inorg. Chem.*, **38**, 1351 (1999).
[4] P. Liu, Y. Liu, Z.X. Lu, J.C. Zhu, J.X. Dong, D.W. Pang, P. Shen, S.S. Qu. *J. Inorg. Biochem.*, **98**, 68 (2004).
[5] T.M. Corneillie, P.A. Whetstone, A.J. Fisher, C.F. Meares. *J. Am. Chem. Soc.*, **125**, 3436 (2003).
[6] S. Aime, M. Botta, M. Fasano, E. Terreno. *Chem. Soc. Rev.*, **27**, 19 (1998).
[7] J.Y. Niu, J.W. Zhao, J.P. Wang. *Inorg. Chem. Commun.*, **7**, 876 (2004).
[8] J.B. Yu, H.J. Zhang, L.S. Fu, R.P. Deng, L. Zhou, H.R. Li, F.Y. Liu, H.L. Fu. *Inorg. Chem. Commun.*, **6**, 852 (2003).

[9] G.J. Isolde, R. Beyer, G. Offord. *Nucl. Med. Biol.*, **24**, 367 (1997).
[10] W.A. Volkert, T.J. Hoffman. *Chem. Rev.*, **99**, 2269 (1999).
[11] M. Neves, L. Gano, N. Pereira, M.C. Costa, M.R. Costa, M. Chandia, M. Rosado, R. Fausto. *Nucl. Med. Biol.*, **29**, 329 (2002).
[12] Y.C. Liang, M.C. Hong, W.P. Su, R. Cao, W.J. Zhang. *Inorg. Chem.*, **40**, 4574 (2001).
[13] J.J. Zhang, S.M. Hu, S.C. Xiang, T.L. Sheng, X.T. Wu, Y.M. Li. *Inorg. Chem.*, **45**, 7173 (2006).
[14] J.P. Costes, G. Novitchi, S. Shova, F. Dahan, B. Donnadieu, J.P. Tuchagues. *Inorg. Chem.*, **43**, 7792 (2004).
[15] J.Q. Gao, D. Li, J. Wang, X.D. Jin, T. Wu, K. Li, P.L. Kang, X.D. Zhang. *J. Coord. Chem.*, **64**, 2234 (2011).
[16] J.Q. Gao, D. Li, J. Wang, X.D. Jin, P.L. Kang, T. Wu, K. Li, X.D. Zhang. *J. Coord. Chem.*, **64**, 2284 (2011).
[17] N.P. Rajesh, K. Meera, C.K. Perumal. *Mater. Chem. Phys.*, **71**, 299 (2001).
[18] T. Egli. *J. Biosci. Bioeng.*, **92**, 89 (2001).
[19] S.J.A. Pope, B.J. Coe, S. Faulkner, E.V. Bichenkova, X. Yu, K. Douglas. *J. Am. Chem. Soc.*, **126**, 9490 (2004).
[20] R. Xu, D. Li, J. Wang, Y.X. Kong, B.X. Wang, Y.M. Kong, T.T. Fan, B. Liu. *Russ. J. Coord. Chem.*, **36**, 810 (2010).
[21] B. Liu, Y.F. Wang, J. Wang, J. Gao, R. Xu, Y.M. Kong, L.Q. Zhang, X.D. Zhang. *Russ. J. Struct. Chem.*, **50**, 880 (2009).
[22] J.Q. Gao, T. Wu, J. Wang, Y. Bai, S.J. Wang, Y.N. Xu, Y. Li, X.D. Zhang. *Russ. J. Coord. Chem.*, **38**, 491 (2012).
[23] L.J. Guggenberger, E.L. Muetterties. *J. Am. Chem. Soc.*, **98**, 7221 (1976).
[24] L.Q. Zhang, T.T. Fan, J. Wang, B. Liu, D. Li, G.X. Han, R. Xu, X.D. Zhang. *Russ. J. Coord. Chem.*, **36**, 389 (2010).
[25] J.Q. Gao, T. Wu, J. Wang, X.D. Jin, D. Li, B.X. Wang, K. Li, Y. Li. *Russ. J. Coord. Chem.*, **37**, 817 (2011).
[26] J. Wang, X.D. Zhang, W.G. Jia, Y. Zhang, Z.R. Liu. *Russ. J. Coord. Chem.*, **30**, 130 (2004).
[27] J. Wang, X.D. Zhang, Y. Zhang, Y. Wang, X.Y. Liu, Z.R. Liu. *Russ. J. Coord. Chem.*, **30**, 850 (2004).